

PIEZOELECTRIC FINITE BEAM ELEMENT WITH FGM CORE FOR MECHATRONIC APPLICATIONS

VLADIMÍR KUTIŠ*, JURAJ PAULECH*, GABRIEL GÁLIK* AND
JUSTÍN MURÍN*

* Department of Applied Mechanics and Mechatronics
Institute of Automotive Mechatronics
Faculty of Electrical Engineering and Information Technology
Slovak University of Technology in Bratislava
Ilkovičova 3, 812 19 Bratislava, Slovak Republic
e-mail: vladimir.kutis@stuba.sk, web page: <http://www.fe.i.stuba.sk>

Key words: Finite Element Method, Piezoelectric Analysis, Functionally Graded Material

Abstract. The paper deals with finite beam element with piezoelectric layers and functionally graded material of core. In the paper homogenization of FGM material properties and homogenization of core and piezoelectric layers is presented. In the process of homogenization direct integration method and multilayer method is used. The concept of transfer functions and transfer constants is used for computation of individual submatrices. Functionality of new FGM finite beam with piezoelectric layers is presented by numerical experiments. Static, harmonic and full transient piezoelectric analysis of FGM beams with piezolayers is presented.

1 MOTIVATION

Modern mechatronic systems are focusing on minimizing size, active vibration control and low energy consumption [1]. To improve performance of mechatronic systems, new materials and technologies are developed - one of them, which found broad application usage is Functionally graded material (FGM). Connection of FGM with piezoelectric materials [2] is very attractive combination of material composition, which can improve functionality of the system.

2 PIEZOELECTRIC CONSTITUTIVE EQUATIONS

Piezoelectric constitutive equations describe the relationship between mechanical and electrical quantities [2, 3]. This relationship is derived in tensor notation, but for practical usage it can be rewritten into matrices notation.

The constitutive equations can be expressed by strain tensor components ε_{kl} and vector components of electric field intensity E_k and has a form

$$\sigma_{ij} = c_{ijkl}^E \varepsilon_{kl} - e_{ijk} E_k \quad (1)$$

$$D_i = e_{ikl} \varepsilon_{kl} + \epsilon_{ik}^E E_k \quad (2)$$

where σ_{ij} are mechanical stress tensor components, D_i are components of electric displacement vector, c_{ijkl}^E are components of stiffness tensor under constant electric intensity, ϵ_{ik}^E are components of permittivity tensor under constant mechanical stress and e_{ijk} are components of piezoelectric modulus tensor.

If we use symmetric properties of individual tensor in constitutive tensor equations, we can rewrite constitutive equations into matrix notation [4]. Then equations (1) and (2) have a form

$$\sigma_p = c_{pq}^E \varepsilon_q - e_{pk} E_k \quad (3)$$

$$D_i = e_{iq} \varepsilon_q + \epsilon_{ik}^E E_k \quad (4)$$

D_i and E_k are vectors with three components, σ_q and ε_q are vectors with six components, matrices c_{pq}^E and c_{pq}^E have dimension 6×6 , matrices d_{iq} and e_{pk} have dimension 3×6 and matrix ϵ_{ik}^E has dimension 3×3 .

3 FGM BEAM WITH PIEZOELECTRIC LAYERS

Straight sandwich beam with core made from functionally graded material (FGM) and top and bottom layers made from piezoelectric material with constant material properties is shown in Fig. 1.

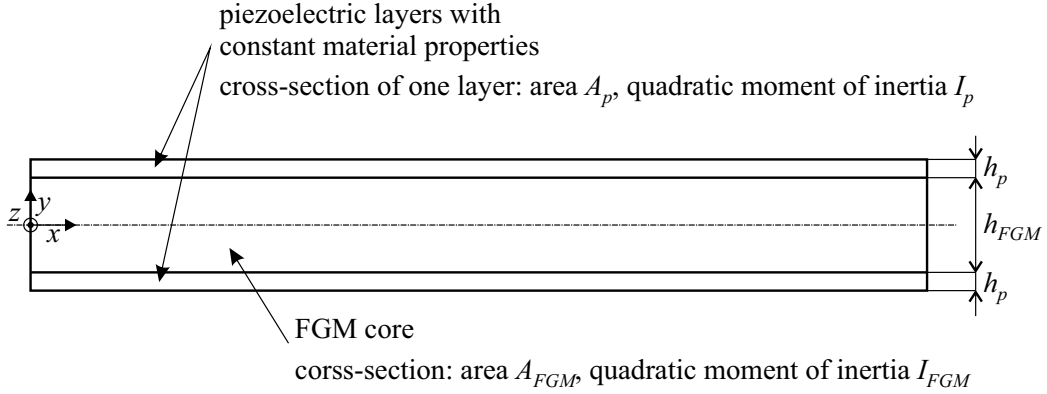


Figure 1: FGM beam with piezoelectric layers

Cross-section of FGM core has height h_{FGM} and depth b , one piezoelectric layer has height h_p and depth b . Cross-section area of FGM core is A_{FGM} and area moment of inertia is I_{FGM} . Cross-section area of one piezoelectric layer is A_p and area moment of inertia is I_p . Length of beam element is L .

3.1 FEM equations for piezoelectric beams with FGM core

2D beam element with piezoelectric layers and FGM core with mechanical and electrical degrees of freedom is shown in Fig. 2.

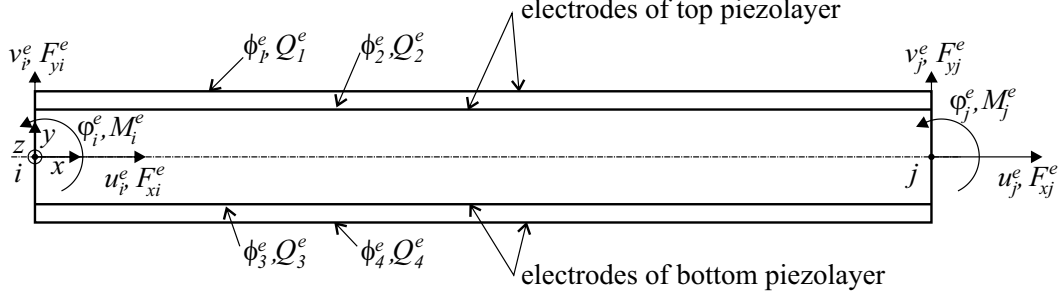


Figure 2: Mechanical and electric DOF in 2D beam element

FEM equations for beam element with piezoelectric layers and FGM core for transient analysis have classical form

$$\begin{bmatrix} \mathbf{M}_{uu}^e & \mathbf{0} \\ \mathbf{0} & \mathbf{0} \end{bmatrix} \begin{bmatrix} \ddot{\mathbf{u}}^e \\ \ddot{\boldsymbol{\phi}}^e \end{bmatrix} + \begin{bmatrix} \mathbf{C}_{uu}^e & \mathbf{0} \\ \mathbf{0} & \mathbf{0} \end{bmatrix} \begin{bmatrix} \dot{\mathbf{u}}^e \\ \dot{\boldsymbol{\phi}}^e \end{bmatrix} + \begin{bmatrix} \mathbf{K}_{uu}^e & \mathbf{K}_{u\phi}^e \\ \mathbf{K}_{\phi u}^e & \mathbf{K}_{\phi\phi}^e \end{bmatrix} \begin{bmatrix} \mathbf{u}^e \\ \boldsymbol{\phi}^e \end{bmatrix} = \begin{bmatrix} \mathbf{F}^e \\ \mathbf{Q}^e \end{bmatrix} \quad (5)$$

Vector of nodal unknowns is defined as

$$\begin{bmatrix} \mathbf{u}^e \\ \boldsymbol{\phi}^e \end{bmatrix} = [u_i \ v_i \ \varphi_i \ u_j \ v_j \ \varphi_j \ \phi_1 \ \phi_2 \ \phi_3 \ \phi_4]^T \quad (6)$$

and vector of nodal loads is defined as

$$\begin{bmatrix} \mathbf{F}^e \\ \mathbf{Q}^e \end{bmatrix} = [F_{xi} \ F_{yi} \ M_i \ F_{xj} \ F_{yj} \ M_j \ Q_1 \ Q_2 \ Q_3 \ Q_4]^T \quad (7)$$

where Q_1 , Q_2 , Q_3 and Q_4 are electric charge on electrodes 1, 2, 3 and 4, respectively.

Individual submatrices are defined by concept of transfer functions and transfer constants and the input parameters for their computation are homogenized material properties in polynomial form. Derivation of individual submatrices is described in [5].

3.2 Homogenization of material properties

Material properties of beam core, which is made from functionally graded material, is defined by:

- volume fractions of fibres $v_f(x, y)$ and by volume fractions of matrix $v_m(x, y)$
- Young's modulus of fibres $E_f(x, y)$ and Young's modulus of matrix $E_m(x, y)$

Both parameters – volume fractions and Young’s moduli, can vary in longitudinal and transversal directions of beam, i.e. in directions x and y .

Effective Youngs modulus of FGM core can be calculated as

$$E_{FGM}(x, y) = v_f(x, y)E_f(x, y) + v_m(x, y)E_m(x, y) \quad (8)$$

Homogenized material properties of FGM core must be calculated separately for axial loading and separately for bending. Homogenized Young’s modulus for axial loading is defined by equation

$$E_{FGM}^{HN}(x) = \frac{\int_{h_{FGM}/2}^{-h_{FGM}/2} bE_{FGM}(x, y)dy}{A_{FGM}} \quad (9)$$

Homogenized Young’s modulus for bending is defined by equation

$$E_{FGM}^{HM}(x) = \frac{\int_{h_{FGM}/2}^{-h_{FGM}/2} by^2E_{FGM}(x, y)dy}{I_{FGM}} \quad (10)$$

Both homogenized Young’s moduli are only function of longitudinal direction x .

The last step in the process of homogenization of material properties of beam is homogenization of FGM core and piezoelectric layers. Young’s moduli for axial loading and bending of whole beam can be calculated using these two equations

$$E^{HN}(x) = \frac{A_{FGM}}{A}E_{FGM}^{HN}(x) + \frac{2A_p}{A}E_p \quad (11)$$

$$E^{HM}(x) = \frac{I_{FGM}}{I}E_{FGM}^{HM}(x) + \frac{2I_p}{I}E_p \quad (12)$$

where A and I is cross-sectional area and area moment of inertial of whole beam cross-section.

4 NUMERICAL EXAMPLE

The effectiveness of new piezoelectric beam element is shown on simple example, where piezoelectric beam is fixed at left end (point i) and right end is free (point j) – see Fig. 3.

Geometry parameters of beam are as follows:

- the length of beam: $L = 100$ mm
- height of FGM core: $h_{FGM} = 10$ mm
- height of piezolayer: $h_p = 1$ mm
- depth of cross-section: $b = 10$ mm

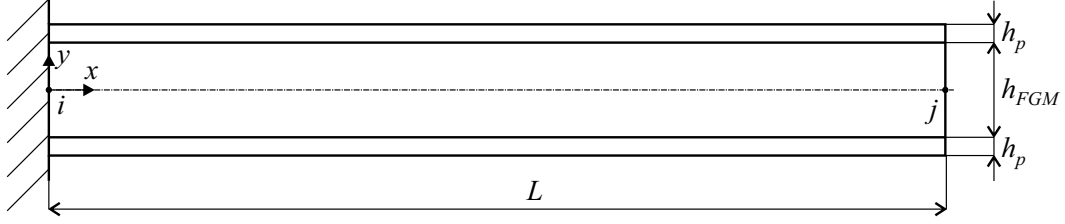


Figure 3: Simple cantilever made of FGM with piezoelectric layers

Beam core is made from FGM material – see chapter 4.1. Upper and bottom layers of the beam are made of piezoelectric material PZT5A. PZT5A is orthotropic material and has following material properties (direction of poling has index 3 – axis y in Fig. 3):

- mechanical properties:
 - Young’s moduli: $E_1 = 61$ GPa, $E_2 = 61$ GPa, $E_3 = 53,2$ GPa
 - Poisson numbers: $\mu_{12} = 0.35$, $\mu_{13} = 0.38$, $\mu_{23} = 0.38$
 - shear moduli: $G_{12} = 22.6$ GPa, $G_{13} = 21.1$ GPa, $G_{23} = 21.1$ GPa
 - density: 7750 kg/m³
- piezoelectric properties: $d_{31} = -171 \times 10^{-12}$ C/N, $d_{33} = 374 \times 10^{-12}$ C/N, $d_{15} = 584 \times 10^{-12}$ C/N, $d_{24} = 584 \times 10^{-12}$ C/N
- relative permittivity: $\epsilon_{11}^\sigma = 1728.8$, $\epsilon_{22}^\sigma = 1728.8$, $\epsilon_{33}^\sigma = 1694.9$

4.1 Computing of homogenized properties

Properties of FGM core are defined by volume fractions of fibre and matrix and by variation of their Young’s moduli. Variation of volume fraction of fibre $v_f(x, y)$ and variation of volume fraction of matrix $v_m(x, y)$ were chosen as planar variation (in coordinates x a y) – see Fig. 4, mathematically they are represented by following functions

$$v_f(x, y) = 1.33333 \times 10^8 x^3 y^2 - 1333.33 x^3 - 2. \times 10^7 x^2 y^2 + 200. x^2 + 40000. y^2 [-] \quad (13)$$

$$v_m(x, y) = 1 - v_f(x, y) [-] \quad (14)$$

Variation of Young’s moduli of fibre and matrix was chosen as linear function longitudinal coordinate x and can be expressed as

$$E_f(x) = 400 - 1000x \text{ [GPa]} \quad (15)$$

$$E_m(x) = 255 - 950x \text{ [GPa]} \quad (16)$$

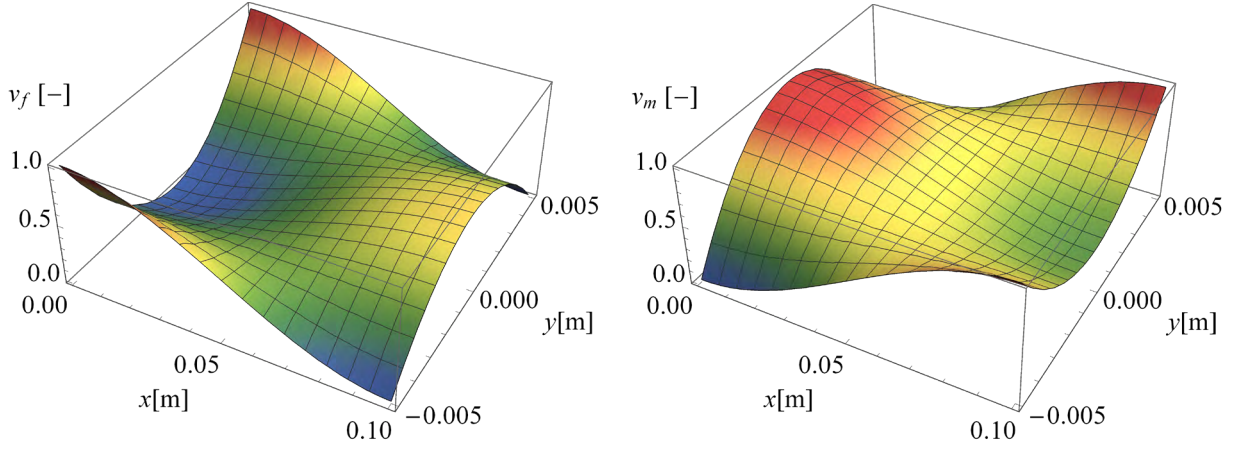


Figure 4: Variation of volume fraction of fibre $v_f(x, y)$ and matrix $v_m(x, y)$

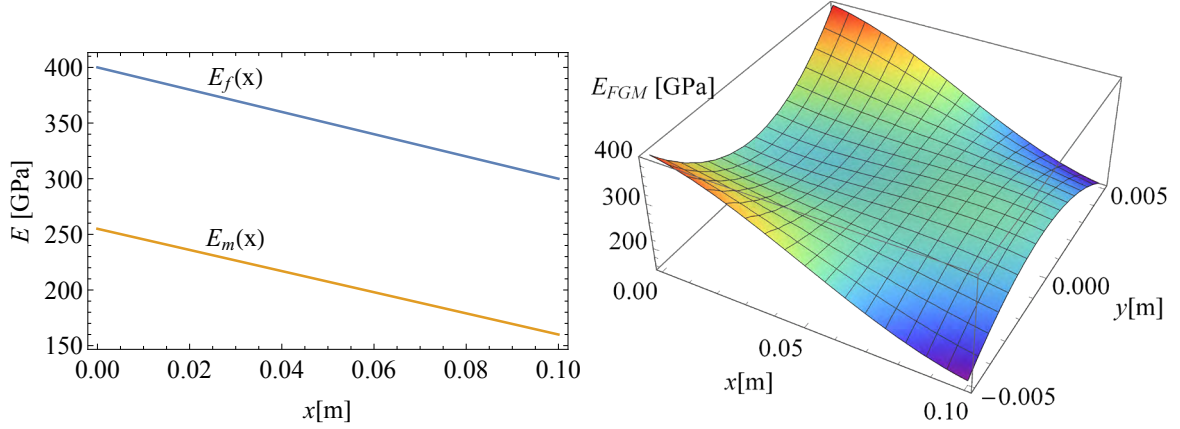


Figure 5: Left – defined variation of $E_f(x)$ and $E_m(x)$, Right – computed variation of effective Young's modulus $E_{FGM}(x, y)$

The variation of $E_f(x)$ and $E_m(x)$ is shown in Fig. 5 Left. Variation of effective Young's modulus $E_{FGM}(x, y)$ is defined by equation (8) and for our example has form

$$\begin{aligned}
 E_{FGM}(x, y) = & - 6.66666 \times 10^9 x^4 y^2 + 66666.7 x^4 + 2.03333 \times 10^{10} x^3 y^2 - \\
 & - 203333. x^3 - 2.9 \times 10^9 x^2 y^2 + 29000. x^2 - 2. \times 10^6 x y^2 - \\
 & - 950. x + 5.8 \times 10^6 y^2 + 255. \text{ [GPa]}
 \end{aligned} \quad (17)$$

This variation of effective Young's modulus is shown in Fig. 5 Right. Homogenized Young's moduli for axial and bending loading of FGM core can be calculated by equations (9) and (10) – $E_{FGM}^{HN}(x)$ and $E_{FGM}^{HM}(x)$. homogenized Young's moduli of whole beam can

be calculated by (11) and (12) and they have form

$$E^{HN}(x) = 11111.1x^4 - 33888.9x^3 + 4833.33x^2 - 966.667x + 303.333 \text{ [GPa]} \quad (18)$$

$$E^{HM}(x) = -33333.3x^4 + 101667.x^3 - 14500.x^2 - 980.x + 342. \text{ [GPa]} \quad (19)$$

Homogenized Young's moduli for axial and bending loading are shown in Fig. 6.

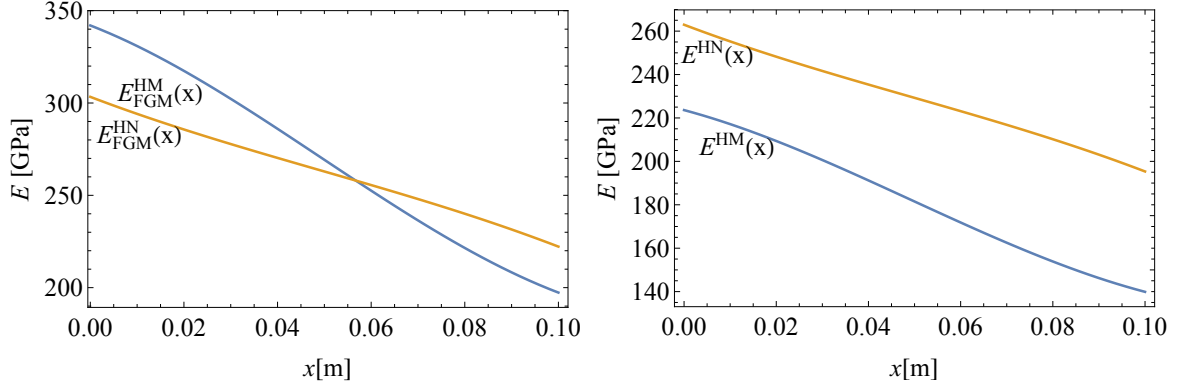


Figure 6: Left – homogenized Young's moduli for axial and bending loading of FGM core, Right – homogenized Young's moduli for axial and bending loading of whole beam.

4.2 Static analysis

Fig. 3 shows simple cantilever made of FGM with piezoelectric layers, which is loaded by transversal force $F = 100$ N at free end – point j . Electrodes on top and bottom piezoelectric layers are short circuited. The goal of analysis is to investigate static responds of structure on prescribed loading and compare the results with different number of elements.

Because the analysis is static and piezoelectric layers are short circuited ($\phi^e = \mathbf{0}$), final FEM equations for deformation and electric charge have form

$$\mathbf{K}_{uu} \mathbf{u} = \mathbf{F} \quad \mathbf{K}_{\phi u} \mathbf{u} = \mathbf{Q}$$

The static analysis of system was performed by FGM beam element with piezoelectric layers. The analysis was performed by 1, 2, 4 and 10 elements – see Fig. 7 Left.

Deformed shape of beam is shown in Fig. 7 Right. Displacement in y direction of free end is $-114.4 \mu\text{m}$. Electric charge on top electrodes for FEM models with different number of elements are summarized in Table 1.

As we can see from obtained results, new FGM beam element with piezoelectric layers is very accurate and effective in static analysis, because variation of material properties of FGM core of beam is directly incorporated into stiffness matrix.

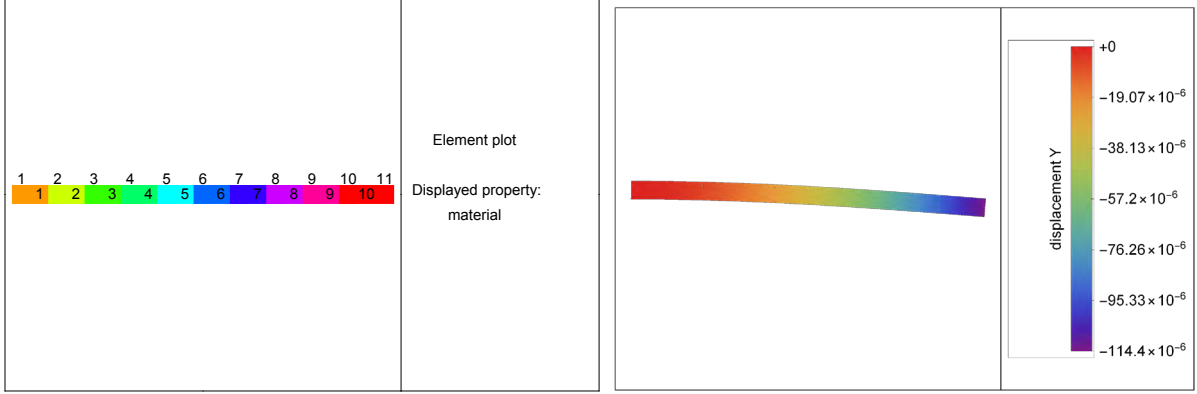


Figure 7: Left – discretized beam with node and element numbers, Right – deformation of beam in [m]

Number of elements	1	2	4	10
$Q_{\text{elem 1}}$ [C]	1.0263×10^{-6}	7.2525×10^{-7}	4.0460×10^{-7}	1.7154×10^{-7}
$Q_{\text{elem 2}}$ [C]		3.0110×10^{-7}	3.2065×10^{-7}	1.5861×10^{-7}
$Q_{\text{elem 3}}$ [C]			2.1883×10^{-7}	1.4560×10^{-7}
$Q_{\text{elem 4}}$ [C]			8.2276×10^{-8}	1.3204×10^{-7}
$Q_{\text{elem 5}}$ [C]				1.1746×10^{-7}
$Q_{\text{elem 6}}$ [C]				1.0137×10^{-7}
$Q_{\text{elem 7}}$ [C]				8.3309×10^{-8}
$Q_{\text{elem 8}}$ [C]				6.2864×10^{-8}
$Q_{\text{elem 9}}$ [C]				3.9732×10^{-8}
$Q_{\text{elem 10}}$ [C]				1.3829×10^{-8}
Q_{SUM} [C]	1.0263×10^{-6}	1.0263×10^{-6}	1.0263×10^{-6}	1.0263×10^{-6}

Table 1: Electric charge on individual electrodes

4.3 Harmonic analysis

Investigated FGM beam with piezoelectric layers was loaded by harmonic force F at the free end (point j – see Fig. 3) with amplitude 100 N with different angular frequency ω . In performed harmonic analysis two different electric boundary conditions are considered:

- short circuit ($\phi^e = 0$)
- open circuit ($Q^e = 0$)

electrode FEM equations for short circuit has form:

$$\mathbf{M}_{uu}\ddot{\mathbf{u}} + \mathbf{C}_{uu}\dot{\mathbf{u}} + \mathbf{K}_{uu}\mathbf{u} = \mathbf{F} \quad \mathbf{K}_{\phi u}\mathbf{u} = \mathbf{Q}$$

FEM equations for open circuit has form:

$$\mathbf{K}_{\phi u}\mathbf{u} + \mathbf{K}_{\phi\phi}\phi = \mathbf{0} \quad \mathbf{M}_{uu}\ddot{\mathbf{u}} + \mathbf{C}_{uu}\dot{\mathbf{u}} + \mathbf{K}_{uu}\mathbf{u} + \mathbf{K}_{u\phi}\phi = \mathbf{F}$$

Harmonic analysis is performed with two different damping conditions:

- without damping
- with Rayleigh damping – the mass proportional Rayleigh damping coefficient is 2×10^{-5} and the stiffness proportional Rayleigh damping coefficient is 2×10^{-5}

Amplitude of y displacement of free end as function of angular frequency ω for all investigated damping and electric conditions are shown in Fig. 8. As we can see from Fig. 8, amplitude-frequency characteristic for open circuit is shift to right – eigenfrequencies of the beam with open circuit are higher.

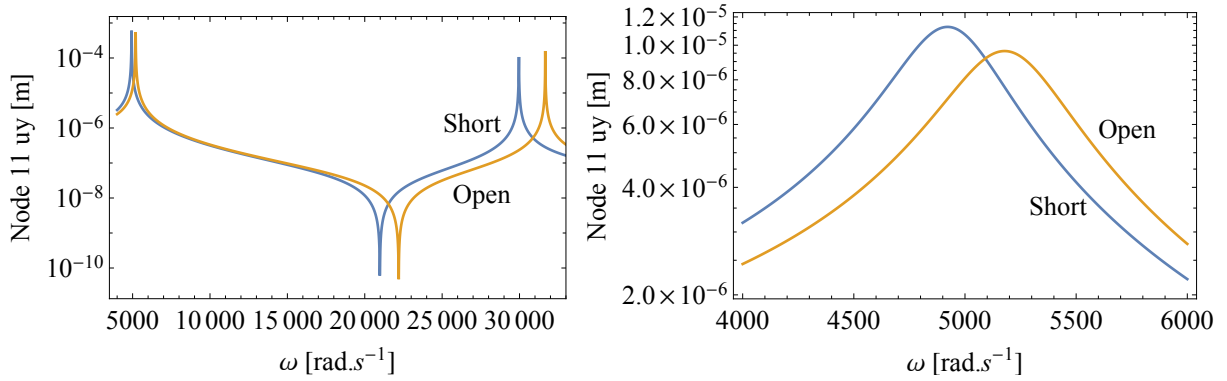


Figure 8: Amplitude-frequency characteristics: Left – without damping, Right – with damping

4.4 Transient analysis

Also transient analysis of investigated FGM beam with piezoelectric layers was performed. Electrodes on top and bottom piezoelectric layers are short circuited. The goal of analysis is to investigate free vibration of structure with considering Rayleigh damping – see Harmonic analysis. FEM equations for displacements and electric charge for transient analysis and for short circuit have form

$$\mathbf{M}_{uu}\ddot{\mathbf{u}} + \mathbf{C}_{uu}\dot{\mathbf{u}} + \mathbf{K}_{uu}\mathbf{u} = \mathbf{F} \quad \mathbf{K}_{\phi u}\mathbf{u} = \mathbf{Q}$$

Initial conditions:

- initial displacement of nodes – initial deformation of system is defined by static analysis – see chapter 4.2
- initial velocity of nodes – all nodes have zero initial velocity

The transient analysis of system was performed by Newmark integration scheme. Total simulation time was 0.01 s and number of equidistant substeps was 100. 1D model of system was discretized by 10 elements – see Fig. 7 Left. Displacement of selected nodes in direction y as function of time are shown in Fig. 9 Left. Time variations of electric charge in top electrode on selected elements are shown in Fig. 9 Right.

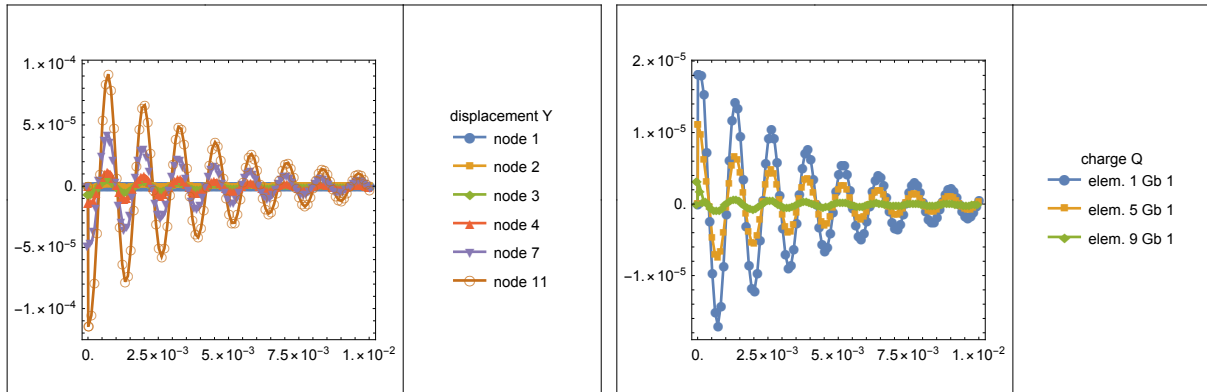


Figure 9: Left – y displacement time variation of selected nodes in [m], Right – charge time variation of top electrodes on selected elements in [C]

5 CONCLUSIONS

The paper presents beam finite element with piezoelectric layers, where core of the beam can be made of FGM materials. Such combination of materials is very attractive for mechatronic applications, because material composition of FGM core can be optimized for design stress state and deformation can be controlled by voltages on electrodes.

ACKNOWLEDGEMENT

This work was supported by the Slovak Grant Agency: VEGA No. 1/0081/18, 1/0102/18 and APVV-0246-12. Authors are also grateful to the HPC Centre at the STU - SIVVP project, ITMS code 26230120002.

REFERENCES

- [1] Preumont, A. *Mechatronics Dynamics of Electromechanical and Piezoelectric Systems*, Springer, (2006).
- [2] Moheimani, S.O.R. and Fleming, A.J.. *Piezoelectric Transducers for Vibration Control and Damping*. Springer, (2006).
- [3] Ballas, R.G.. *Piezoelectric Multilayer Beam Bending Actuators*. Springer, (2007).
- [4] Nye, J.F.. *Physical Properties of Crystals*. Oxford, (2011).
- [5] Kutíš, V, Paulech, J., Murin, J. and Galik, G. *Analysis of Piezoelectric Beams for Smart Structures*. APCOM 2018, (2018).